Effects of ponderomotive forces on "electroelastic" membrane instability (electroporation) and voltage gating

Michael B. Partenskii, Gennady V. Miloshevsky and Peter C. Jordan
Department of Chemistry, Brandeis University, Waltham, MA, USA

ABSTRACT

The electric energy associated with thickness (h) fluctuations of a low dielectric (ε=2) membrane slab sandwiched between two solvent domains (ε_{solv}) under an applied voltage V is analyzed using the Finite Difference (FD) 2-D algorithm [1]. Unlike the 3D-FD approach used in DelPhi, we are restricted to analyzing cylindrically symmetric perturbations but permitted a wider choice of perturbation profiles (see [2] and references therein). We consider membrane thickness fluctuations of either Gaussian or Hertzian profiles (the latter prompted by a solution for a "pinned" membrane). We sample a range of εsolv, from infinity (perfect conductor) to ε = 40 (partially immobilized water). Elastic energy is analyzed in the smectic bilayer model with possible membrane mode softening [3]; for each u, the total electroelastic energy, W(u,d), is optimized with respect to the decay length of the fluctuations. This analysis shows that ponderomotive forces can trigger membrane instability at electric fields F~0.6-0.7 V/nm, slightly lower than predicted by molecular dynamics [4-6] but still larger than the experimental values, typically 0.1-0.3 V/nm. The effect of thickness fluctuations partially stabilizing charged groups embedded in a membrane is also analyzed. A possible role for this effect in voltage gating is proposed.

I. INTRODUCTION

Membrane electroporation and voltage gating of ion channels are two examples of biophysical phenomena where comparatively low electric fields corresponding to voltages of a few hundred millivolts have major physical consequences. Theoretical explanation of both phenomena is a challenging problem. For example, a simple electroelastic model of membrane instability (Crowley, see [2] for details) predicted the critical voltage for membrane breakdown 3-5 times larger than observed values. The attempts [4-6] to simulate this phenomena did not bring clarity because voltages comparable to the Crowley values have been used (see [2]).

The problem of Voltage gating became especially puzzling after MacKinnon's [7-10] observations that the highly charged voltage sensor might be positioned in the hydrophobic membrane region and cross the membrane in response to a comparatively weak electric field. One reason for skepticism was the huge "image force" barrier for a charge crossing the membrane.

A more detailed understanding of these phenomena can be gained by analyzing the electric coupling between the voltage and the charges on one hand and membrane fluctuations on the other.

This coupling results from the ponderomotive force caused by the strong non-uniformity of the electric field at the membrane-water interface, which promotes membrane thickness fluctuations, expressed as h(r) = h_0[1+2z(r)], where z(r) describes the thickness perturbation profile. This force competes with the opposing elastic force, and together they define the total potential (electroelastic) energy of the fluctuations.

We have considered two types of trial functions to describe the shapes of the thickness fluctuations (dimples), Gaussian z(r) ~ u exp[-(r/λ)2] and Hertzian z(r) ~ u Kei[r/λ] (prompted by the solution to the Hertz "pinned" membrane problem [11]), with λ the fluctuation decay length (Fig. 1). It turned out that Hertzian shapes in most of the cases provide better optimization, and in the following discussion we only deal with them.

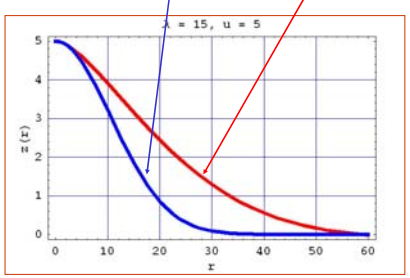

Fig. 1 Gaussian & Hertzian profiles

Hertzian shapes are better trial functions for optimizing the total energy and are used in what follows.

II. MEMBRANE FLUCTUATIONS IN AN ELECTRIC FIELD AND THEIR POSSIBLE ROLE IN ELECTROPORATION

2.1 Effects due to large local thickness fluctuations (dimples)

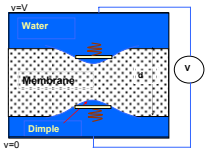

Fig. 2 Computational cell used for solving the electrostatic problem is a cylinder of radius R = 10 nm. Dimples in 2D analysis are axially symmetric. Springs symbolize the elastic energy associated with the dimples.

Electrostatic calculations were carried out for membrane thicknesses, h, from 2.1 to 3 nm, decay parameters, λ, from .5 to 2 nm and amplitudes, u, from 0 to 1 nm. For dioleoylphosphatidylcholine (DOPC) membranes the natural Hertz decay length is λ_0 ~ .75 nm.

Elastic energy – local model: The total deformational energy, Wd, is the sum of independent stretching (W_s) & bending (W_b) terms, where

$$W_s = 4\pi E_s/h^2 \int z(r)^2\, r\,dr, \qquad W_b = \pi K_c \int (\nabla^2 z(r))^2\, r\,dr \qquad (2.1)$$

E_s and K_c are stretching and bending elastic moduli respectively.

Total energy: Local treatment of elastic energy

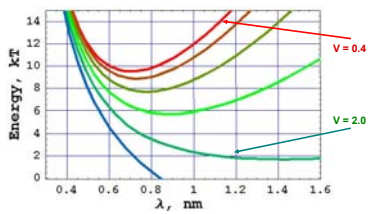

Fig. 3 Total (elastic & electrostatic) energy of a Hertzian dimple of u = 0.5 nm for voltages from 0.4 to 2.4 V in 0.4 V steps; this u corresponds to ~30% local thinning.

Elastic energy – non-local model: Here the total deformational energy no longer separates neatly into stretching and bending terms. Instead non-locality is described as a wave vector (**q**) dependence of the elastic moduli. Consider a symmetric fluctuation u(**q**, **ρ**),

$$u(\mathbf{q},\boldsymbol{\rho}) = \Sigma_q\, u_q \exp[-i\mathbf{q}\cdot\boldsymbol{\rho}], \qquad (2.2)$$

with **ρ** the radius vector, $\mathbf{q} = \{q_x, q_y\}$ a 2-D wave vector ($2\pi/\xi_{max} \le q \le 2\pi/\xi_{min}$), $\xi max = A^{1/2}$ and $\xi_{min} = L$ (ξ is the perturbation's wavelength). Here A is the membrane surface area and *L* a typical lipid head group dimension. The total deformational energy is [3]

$$W_d = 2\Sigma_q\, (E_s\, |u_q|^2 h_0^2)\, f(q,\alpha), \qquad (2.3)$$

where $f(q,\alpha)$ is the mode energy. It has two characteristic regions, a long wavelength domain ($2\pi/q = \xi \ge$ 2-3 h) corresponding to macroscopic membrane constants and the short wavelength region ($\xi <$ h) with modes softened compared to the macroscopic limit. In what follows we introduce a single "softening factor" r assuming that elastic constants E_s and K_c are reduced by the same factor r in the short ξ limit (see [3]). Non-local behavior may be described in terms of *effective* local elastic constants which depend upon the fluctuating dimple's decay length, λ. We found this dependence can be approximated by the function

$$f(\lambda) = r^{-1} + (1 - r^{-1})/(1 + \exp[(\lambda - \lambda_s)/\varsigma]), \qquad (2.4)$$

so that $\{E_s(r,\lambda), K_c(r,\lambda)\} \sim f(\lambda)\,\{E_s, K_c\}$; for DOPC reasonable values for the parameters (λ_s and ς) are $\lambda s \sim 0.8\ h_0$; $\varsigma \sim 0.3\ h_0$. Then $E_s(r,\lambda)$ and $K_c(r,\lambda)$ can be substituted in the **local** expression, Eq. 2.1, which reasonably approximates the non-local energy with the corresponding value of r. In Fig. 4 we set r = 2, a moderate softening factor, compared to that suggested in [3] (r ~ 10) to account for the intermediate voltage instability of small harmonic perturbations.

Total energy: Non-local treatment of elastic energy

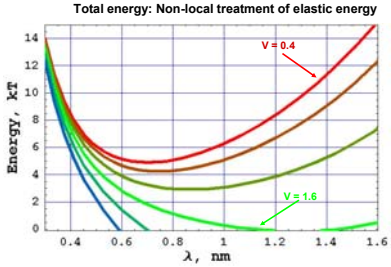

Fig. 4 Total energy of a Hertzian dimple of u = 0.5 nm for voltages from 0.4 to 2.4 V in 0.4 V steps; this u corresponds to ~ 30% local thinning (softening factor, r = 2).

Relative to the local limit, instabilities (Energy → 0) are shifted towards smaller V and shorter λ. Instabilities start at V ~1.6 V (Fig. 4) & ~2.1 V (Fig. 3).

2.2 Some consequences and future directions

Membrane electroporation may be preceded by large local fluctuations, which perturb lipid packing and sharply increase water penetration, thus promoting pore formation. Our approach can't describe pore formation since the membrane loses its integrity and elastic theory no longer applies, but the ponderomotive mechanism permits preliminary observations relative to an instability's voltage dependence. Assuming a characteristic time for the appearance of large fluctuations is

$$\tau(V) = \tau_r Exp[-\delta F_{min}(V)/kT]$$

where δFmin(*V*) is the total dimple formation energy optimized with respect to its shape parameter λ. Relative to the critical voltage *V** (where total dimple formation energy → 0), Table 1 illustrates how lowering voltage affects the "waiting time," τ(V)/τ(V*), for spontaneous occurrence of large fluctuations in DOPC membranes described in the local (r = 1) and non-local (r > 1) approximations.

Table 1: Voltage dependence of relative "waiting time," τ(V)/τ(V*), on the softening factor r (r=1 corresponds to the local model)

r	V* (Volts)	τ(V)/τ(V*)		
		V/V*= 0.25	0.5	0.75
1	~2.2	2247	849	108
2	~1.6	52.5	32.4	9.1
3	~1.2	18.1	11.5	4.8

This analysis rationalizes why modeling electroporation [4-6] is carried out at voltages near the critical values. Insignificant voltage decreases can dramatically increase modeling time. This analysis is also relevant to the experimental observation that membrane breakdown depends on the duration of the electric pulses [12]. However, more consistent analysis requires taking some dynamic aspects of membrane relaxation into consideration. More detailed analysis should treat for both uniform and local membrane perturbation. Apparently, at the large voltages considered in Refs. [4-6] and near to *V**, local fluctuations and the corresponding membrane breakdown are a more efficient stress relaxation mechanism than uniform membrane compression-stretching. This would explain why the uniform membrane deformation (e.g., a noticeable increase in the area per lipid due to the electrostatic pressure) was not observed in the simulations [4-6]. One can expect that for smaller *V* and much longer "waiting times ", both factors will matter.

III. EFFECT OF LOCAL FLUCTUATIONS ON THE ELECTRICAL IMAGE BARRIER

Deformational fluctuations affect membrane stability under an applied voltage. Here we consider a complementary problem, stability in the presence of fixed charges.

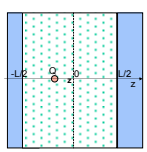

Fig. 5: Charge Q in a planar bilayer

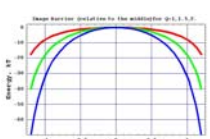

Fig. 6: Image barrier for a 3 nm wide planar membrane slab (ε_M = 2 & ε_W = 80). It greatly destabilizes charges in a bilayer.

Effects of membrane deformability on image barriers

In reality, membranes are deformable; ponderomotive forces attracting water to the charge compete with the elastic energy of perturbation. Here we treat charges fixed at different distances from the edge of membrane (z is a "reaction coordinate") and analyze the perturbation energy using the electrostatic 2D analysis and the smectic elastic model.

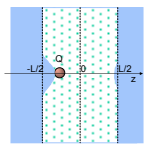

Fig. 7: Cartoon of a charge in a deformable membrane.

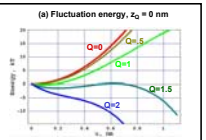

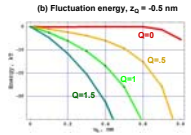

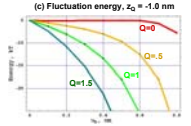

Fig. 8: Effect of fluctuation amplitude on "stabilization energies." **a**: Charges fixed at mid-membrane and energy optimized with respect to λ; values of Q included in the figure. For small Q there is a wide range of stability. At Q = 1.5, the system is unstable for u > 0.6. For Q = 2, it is absolutely unstable. **b & c**: Charges off-center and energy optimized with respect to λ_L, λ_R and u_R. For the off-center ions there is almost always a powerful net driving force promoting dimple growth.

While this picture is most simplified, it demonstrates possible importance of membrane deformation in stabilizing embedded charges. In particular we consider a "molecular ion" (the sphere in Fig. 7) of effective diameter 6 Å and assume the dimple can't "penetrate" the hard shell surrounding the ion.

Table 2: Stabilization energy, E_{st}, for the "molecular ion" for two locations and three values of Q, defined relative to the image barrier for an ion at the same distance from the center of an unperturbed planar slab.

z_Q	E_{st}/kT Q=1	E_{st}/kT Q=1.5	E_{st}/kT Q=2
-1.0 nm	-19.4	-44.6	-79.9
-0.5 nm	-25.4	-68.2	-128.7

Table 3: Effect of membrane deformation on the energy barrier ΔW between the two off-center ion locations (z_Q = -1 & 0.5 nm) for three Q values.

Model	Δ W/kT Q=1.	Δ W/kT Q=1.5	Δ W/kT Q=2
Planar slab	16.1	36.2	64.4
Perturbed membrane	9.6	12.4	15.6

IV. CONCLUSIONS

1. The "image" barrier is greatly reduced. Ponderomotive effects significantly stabilize membrane charges relative to the classical image barrier estimates.
2. The decrease in the total energy with increasing dimple amplitude (Fig. 8a, for Q ≥1.5) shows that interaction between a charge "pinned" in the membrane and a "dimple" can lead to local breakdown eventually forming a water "droplet" surrounding the charge.
3. For further analysis, interaction of water with the hydrophobic membrane interior must be included.
4. To be applicable to voltage gating, the real charge distribution of the voltage sensor must be considered. This requires a 3D treatment of the electrostatic problem which can be achieved by using a modified version of DelPhi (see neighboring poster [2] and references therein).

REFERENCES

1. Miloshevsky et al., J. Comp. Phys., 212:25 [2006]
2. Jordan, Partenskii and Rocchia, this meeting, neighboring poster.
3. Partenskii, Dorman and Jordan, J. Chem. Phys., 109: 10361 [1998]
4. Tieleman, BMC Biochemistry, 5:10 [2004]
5. Tarek, Biophys. J., 88:4045 [2005]
6. Gurtovenko and Vattulainen, J. Am. Chem. Soc., 127:17570 [2005]
7. Jiang et al., Nature, 423:33 [2003]
8. Jiang et al., Nature, 423:42 [2003]
9. Lee et al. PNAS, 102:15441 [2005]
10. Long et al., Science, 309:897 [2005]
11. Jordan, Miloshevsky,Partenskii In "Interfacial Catalysis" (Volkov Ed.) p. 493, Marcel Dekker, [2003]
12. Weaver and Chizmadzhev, Bioelectrochem. Bioenerg., 41:135 [1996]; Melikov,et al., Biophys J., 80:1829 [2001]

ACKNOWLEDGEMENT

Supported by a grant from the National institutes of Health, GM-28643